Published in final edited form as:
Exp Eye Res. 2012 June ; 99: 1–16. doi:10.1016/j.exer.2012.03.019.

The combination of IGF1 and FGF2 and the induction of excessive ocular growth and extreme myopia

Eric R. Ritchey[1,#], **Christopher P. Zelinka**[2], **Junhua Tang**[3], **Jun Liu**[3], and **Andy J. Fischer**[2,*]

[1]College of Optometry, The Ohio State University, Columbus, Ohio 43210

[2]Department of Neuroscience, College of Medicine, The Ohio State University, Columbus, Ohio 43210

[3]Department of Biomedical Engineering, The Ohio State University, Columbus, Ohio 43210

Abstract

Different growth factors have been shown to influence the development of form-deprivation myopia and lens-induced ametropias. However, growth factors have relatively little effect on the growth of eyes with unrestricted vision. We investigate whether the combination of insulin-like growth factor 1 (IGF1) and fibroblast growth factor 2 (FGF2) influence ocular growth in eyes with unrestricted vision. Different doses of IGF1 and FGF2 were injected into the vitreous chamber of postnatal chicks. Measurements of ocular dimensions and intraocular pressure (IOP) were made during and at the completion of different treatment paradigms. Histological and immunocytochemical analyses were performed to assess cell death, cellular proliferation and integrity of ocular tissues. Treated eyes had significant increases in equatorial diameter and vitreous chamber depth. With significant variability between individuals, IGF1/FGF2-treatment caused hypertrophy of lens and ciliary epithelia, lens thickness was increased, and anterior chamber depth was decreased. Treated eyes developed myopia, in excess of 15 diopters of refractive error. Shortly after treatment, eyes had increased intraocular pressure (IOP) which was increased in a dose-dependent manner. Seven days after treatment with IGF1 and FGF2 changes to anterior chamber depth, lens thickness and elevated IOP were reduced, whereas increases in the vitreous chamber were persistent. Some damage to ganglion cells was detected in peripheral regions of the retina at 7 days after treatment. We conclude that the extreme myopia in IGF1/FGF2-treated eyes results from increased vitreous chamber depth, decreased anterior chamber depth, and changes in the lens. We propose that factor-induced ocular enlargement and myopia result from changes to the sclera, lens and anterior chamber depth.

Keywords

myopia; retina; IGF1; FGF2; amacrine cell

[*]**corresponding author:** Andy J. Fischer, Department of Neuroscience, Ohio State University, College of Medicine, 4190 Graves Hall, 333 W. 10th Ave, Columbus, OH 43210-1239, USA. Telephone: (614) 292-3524; Fax: (614) 688-8742; fischer.412@osu.edu.
[#]**Current Address:** Eric Ritchey, Principal Research Optometrist, Vistakon, Johnson & Johnson Vision Care, Inc., Research and Development, 7500 Centurion Parkway, W-2A Jacksonville, FL, 32256, USA

1. Introduction

Eye growth is a complex, well-coordinated process with an endpoint of minimal to no refractive error; a process known as emmetropization. In the vertebrate species studied thus far, the eyes have significant refractive error at the time of birth (Wallman and Winawer 2004). During adolescence, the eye grows so that the length of the vitreous chamber precisely matches the combined refractive power of the lens and cornea to eliminate refractive error. Humans undergo active emmetropization; however we differ from other vertebrate species in that a significant number of individuals fail to properly emmetropize and, consequently, develop myopia (nearsightedness). Myopia commonly results from elongation of the vitreous chamber which is determined by the growth of the sclera; the connective tissue sheath of the eye.

In animal models, attenuated clear vision has been shown to cause excessive ocular growth and myopic refractive errors. This model is known as form-deprivation myopia (FDM). The requirement for normal vision is well-conserved across species including chicks, marmosets, tree shrews, mice, monkeys, and rabbits (Guo et al. 1995; Norton 1990; Tejedor and de la Villa 2003; Troilo and Judge 1993; Wallman et al. 1978; Wallman and Winawer 2004; Wiesel and Raviola 1977). It is currently believed that the retina detects defocus cues and liberates factors that accelerate or decelerate the growth of the sclera (reviewed by Wallman and Winawer 2004). The retina-derived factors that regulate eye growth remain poorly understood. Several peptide and amino acid-derived neurotransmitters in the retina have been implicated as growth-regulators in animal models of myopia (reviewed by Wallman and Winawer 2004). In the chick model system, the most promising candidate for a retina-derived signal that regulates ocular growth is glucagon peptide. We have reported that the glucagon-expressing retinal amacrine cells (GACs) respond to growth-slowing visual stimuli (plus-defocus and recovery from FDM) by up-regulating the immediate early gene Egr1 (Fischer et al. 1999a). By contrast, the GACs respond to growth-accelerating visual cues by down-regulating Egr1 (Fischer et al. 1999a). Additional reports have indicated that growth-guiding visual cues influence retinal levels of glucagon mRNA (Buck et al. 2004), and that agonists and antagonists to the glucagon receptor influence rates of ocular growth in form-deprived and lens-treated eyes (Feldkaemper and Schaeffel 2002; Fischer et al. 2008b; Vessey et al. 2005). Recent studies have indicated that exogenous insulin and Insulin-like growth factor 1 (IGF1) can exacerbate the excessive ocular growth that results from form-deprivation, and can counter-act the growth-slowing effects of glucagon (Feldkaemper et al. 2009; Zhu and Wallman 2009). Injections of insulin and IGF1 into eyes with unrestricted vision increased the axial length of eyes with unrestricted vision, however increases in vitreous chamber depth contributed relatively little to total increases in axial length (Feldkaemper et al. 2009; Zhu and Wallman 2009). In addition, a recent study has identified genetic associations between IGF1 polymorphisms and high-grade myopia in humans (Metlapally et al. 2010), consistent with the hypothesis that insulin and IGF1 have important roles in regulating rates of ocular growth and the pathogenesis of myopia.

The mechanisms underlying insulin/IGF1-induced changes in ocular growth remain uncertain. The identity of the cells that express receptors, signaling pathways and the types of cells that directly respond to insulin and IGF1 have recently been studied. Feldkaemper and colleagues (2009) reported that the expression of the immediate early gene Egr1 near the middle of the INL suggests that the Müller glia may respond to insulin. We have reported that intraocular injections of insulin selectively stimulate the Müller glia to accumulate Egr1, cFos and low levels of pERK, whereas retinal neurons do not appear to respond (Fischer et al. 2009a). By comparison, IGF1 stimulates the Müller glia to accumulate p38 MAPK and cFos, whereas retinal neurons do not appear to respond (Fischer et al. 2010). In addition, we have reported that insulin and IGF1 stimulate the reactivity of

microglia and a novel type of glial cell, termed Non-astrocytic Inner Retinal Glial (NIRG) cells (Fischer et al. 2009a; Fischer et al. 2010), and stimulate the proliferation of retinal progenitors in the circumferential marginal zone (CMZ) and non-pigmented epithelium of the pars plana (Fischer et al. 2002a; Fischer and Reh 2000; Fischer and Reh 2003). Collectively, these findings indicate that the effects of insulin and IGF1 are subtly different, but are centered on the retinal glia. The possibility remains that insulin and IGF1 act at extra-retinal tissues to influence rates of ocular growth.

Another growth factor that may be involved in regulating ocular growth is fibroblast growth factor (FGF). Rohrer and Stell (1994) reported that low doses (<5ng) of FGF2 inhibit FDM, whereas high doses (~300ng) of FGF1 cause retinal degeneration that includes the loss of photoreceptors and detachment from the RPE (Rohrer and Stell 1994). However, it has been our experience, and that of others (Chaum 2003; Hicks 1998; LaVail et al. 1998; Valter et al. 1998), that FGF is potently neuroprotective for different types of retinal cells including photoreceptors and that these neuroprotective actions may be elicited through the Müller glia (Fischer et al. 2009a). Through the course of studies into effects of IGF1 and FGF2 on retinal glia and neuronal survival, we noticed that treated eyes appeared significantly larger than contra lateral control eyes. Thus, the purpose of the current study was to investigate how the combination of IGF1 and FGF2 influence ocular growth. Some of this work has been presented at the 13th International Myopia Conference (Tuebingen, Germany) (Tarutta et al.).

2. Methods and materials

2.1. Animals

The use of animals in these experiments was in accordance with the guidelines established by the National Institutes of Health, the ARVO Statement for the Use of Animals in Ophthalmic and Vision Research, and the Ohio State University. Newly hatched leghorn chickens (*Gallus gallus domesticus*) were obtained from the Department of Animal Sciences at the Ohio State University. Postnatal chicks were kept on a cycle of 12 hours light, 12 hours dark (lights on at 8:00 AM). Chicks were housed in a stainless steel brooder at about 25°C and received water and chick starter (Purina, St. Louis, MO) *ad libitum*.

2.2. Intraocular injections and paradigms

Prior to injections, chicks were anesthetized by inhalation of 2.5% isoflurane in O_2 at a flow rate of 1.5 L/min. Injections were made with a 25 μl Hamilton syringe and 26G needle with a cutting tip. The needle was consistently inserted into the dorsal quadrant of the vitreous chamber thought the pars plana and dorsal eye lid, which was sterilized with iodine solution. Daily injections were made between 1 and 2 pm. For all experiments, the left eyes of chicks were injected with the “test” compound and the contra-lateral eyes were injected with vehicle as a control. Compounds were injected in 20 μl sterile saline with 0.05 mg/ml bovine serum albumin added as carrier. Compounds included insulin (1 μg (175 pmol) per dose; Sigma-Aldrich, St. Louis, MO), recombinant human IGF1 (50 to 800 ng (6.5 to 104.6 pmol) per dose; R&D Systems, Minneapolis, MN), recombinant bovine FGF2 (200ng (12.3 pmol) per dose; R&D Systems). Estimated initial maximum concentrations of factors in the vitreous included 1 μg insulin = 653 nM, 50 ng IGF1 = 24 nM, 100 ng IGF1 = 44 nM, 200 ng IGF1 = 88 nM, 800 ng IGF1 = 352 nM, 100 ng FGF2 = 23 nM and 200 ng FGF2 = 46 nM. At P7 serum levels of IGF1 are about 18 ng/ml (Lu et al. 2007). Thus, assuming a volume of liquid vitreous of 200 μl, a dose of 200ng IGF would result in an initial maximum concentration within the vitreous which is about 50-fold above serum levels. Combining the volumes of gel vitreous with liquid vitreous, a dose of 200ng IGF1 would result in an initial maximum concentration within the vitreous which is about 10-fold above serum levels. Two

μg of BrdU was included with each injection (treatment and control) to label proliferating cells through the course of the experiments. Control eyes were injected with vehicle (saline added with 0.05 ml/ml bovine serum albumin and BrdU).

Injections and measurement paradigms were as follows: Paradigm 1 - data in Figures 2 and 3: Beginning at P5 and ending at P7, eyes (n=6) were injected daily with vehicle or 800 ng IGF1 and 200 ng FGF2. At P8, 24 hours after the last injection, retinoscopy was performed, chicks were sacrificed, eyes enucleated and photographed, and tissues processed for immunolabeling. Paradigm 2 - data in Figures 4a–d,g, 5a–f, 6a,b,f and 7: Beginning at P5 and ending at P8, eyes (n=10) were injected daily with vehicle or 200 ng IGF1 and 200 ng FGF2. At P9, 24 hours after the last injection, retinoscopy was performed, ultrasound measurements were made, chicks were sacrificed, eyes enucleated and photographed, and tissues processed for histology and immunolabeling. Paradigm 3 - data in Figures 4e,f,h, 5g–l, and 6c–e,g: Beginning at P5 and ending at P8, eyes (n=10) were injected daily with vehicle or 200 ng IGF1 and 200 ng FGF2. At P16, 7 days after the last injection, retinoscopy was performed ultrasound measurements were made, chicks were sacrificed, eyes enucleated and photographed, and tissues processed for histology. Paradigm 4 - data in Figure 8 (and for data not shown): Beginning at P5 and ending at P8, eyes (n=6) were injected daily with 300 ng IGF1 alone, 200 ng FGF2 alone, 1 μg insulin + 200 ng FGF2, 50 ng IGF1 + 200 ng FGF2, 200 ng IGF1 + 200 ng FGF2, or 300 ng + 200 ng FGF2. At P11, 24 hours after the last injection, measurements of IOP were made, and for the combination of 300 ng IGF1 and 200 ng FGF2 measurements were also made at P18, 7 days after the last injection. Paradigm 5 - data in Figure 9: Beginning at P5 and ending at P8, eyes (n=6) were injected daily with vehicle or 200 ng IGF1 and 200 ng FGF2. Beginning at P5 and ending at P9, control and treated eyes were measured with A-scan ultrasound, refractive error assessed and a tonometer (described below). Measurements of IOP were made at the same time of day and before the injections. Paradigm 6 - data in Figure 10: Beginning at P5 and ending at P9, eyes (n=6) were injected daily with vehicle or 100 ng IGF1 and 100 ng FGF2. At P9, 24 hours after the last injection, retinoscopy was performed, ultrasound measurements were made, chicks were sacrificed, eyes enucleated and photographed, and tissues processed for histology and immunolabeling.

2.3. Reverse transcriptase PCR

To ensure that sufficient amounts of purified RNA were obtained, tissues were pooled from two P7 chicks. Ocular tissues were dissected in cold (~4°C) Hanks' Balanced Salt Solution added with 3% D-glucose and 0.01 M HEPES (HBSS+). Isolated tissues included (1) retina that was devoid of pigmentation (retina with adherent RPE was excluded), (2) choroid with adherent RPE, (3) ciliary body including fragments of lens capsule, (4) lens fiber cells, and (5) sclera – both cartilaginous and fibrous layers. Following dissection, isolated tissues were rinsed in cold HBSS+ to reduce the possibility of contamination of other tissues. Tissues were placed in 1.5 ml of Trizol Reagent (Invitrogen; Carlsbad, CA) and total RNA was isolated according to the Trizol protocol and resuspended in 50 μl RNAse free water. Genomic DNA was removed by using the *DNA FREE* kit provided by Ambion (Austin, TX). cDNA was synthesized from mRNA by using Superscript^{tm} III First Strand Synthesis System (Invitrogen) and oligo dT primers according to the manufacturer's protocol. PCR primer sequences and predicted product sizes are listed in table 1. Primers were designed by using the Primer-BLAST primer design tool at NCBI (http://www.ncbi.nlm.nih.gov/tools/primer-blast/). PCR reactions were performed by using approximately 10 ng cDNA template, Platinum^{tm} Taq (Invitrogen) or TITANIUM^{tm} Taq (Clontech; Mountain View, CA) and an Eppendorf thermal cycler. Following a denaturing step (1 min at 94°C), 40 cycles of 1 min at 60–67.4°C for annealing, 1 min at 68°C for elongation, and 30 sec at 94°C for denaturing were run. PCR products were run on a 1.2%

agarose gel to verify the predicted product sizes, products were excised from the gels, extracted, purified (Qiaex II kit, Qiagen; Valencia, CA), and sequenced to verify the identity of the products. Control reactions were performed using all components with the exception of the reverse transcriptase to exclude the possibility that primers were amplifying genomic DNA.

2.4. Fixation, sectioning and immunocytochemistry

Tissues were fixed, sectioned and immunolabeled as described previously (Fischer et al. 2008a; Fischer and Omar 2005). Working dilutions and sources of antibodies used in this study are listed in table 2. Antigen retrieval was used to permit immunolabeling for BrdU and PCNA, sections were washed for 7 minutes in 4M HCl. Secondary antibodies included donkey-anti-goat-Alexa488, goat-anti-rabbit-Alexa488, goat-anti-mouse-Alexa488/568, rabbit anti-goat Alexa488 and goat-anti-mouse-IgM-Alexa568 (Invitrogen) diluted to 1:1000 in PBS plus 0.2% Triton X-100.

We evaluated the specificity of primary antibodies by comparison with published examples of results and assays for specificity. None of the observed labeling was due to non-specific labeling of secondary antibodies or autofluorescence because sections labeled with secondary antibodies alone were devoid of fluorescence. Secondary antibodies included goat-anti-rabbit-Alexa488/568/647 and goat-anti-mouse-Alexa488/568/647 (Invitrogen) diluted to 1:1000 in PBS plus 0.2% Triton X-100.

2.5. Terminal deoxynucleotidyl transferase dUTP nick end labeling (TUNEL)

To identify dying cells that contained fragmented DNA we used the TUNEL method. We used an *In Situ* Cell Death Kit (TMR red; Roche Applied Science; Indianapolis, IN), as per the manufacturer's instructions.

2.6. Retinoscopy

We used trial lenses and streak retinoscopy to measure refractive error in control and treated eyes, similar to previous reports (Fischer et al. 1999a). Retinoscopy was performed by one individual to prevent inter-individual variability. Measurements of refractive error were made at the termination of each experiment, one day after the last intraocular injection.

2.7. Measurement of Intraocular Pressure (IOP)

A TonoLab^{tm} tonometer was used to measure IOP. The device was used with the factory-set calibration for rat eyes, similar to recent reports (Morrison et al. 2009; Pease et al. 2010). *In vivo* measurements of IOP were made at the termination of each experiment, at one day or 7 days after the last intraocular injection. Measurements of IOP were made consistently at the same time of day.

2.8. Microscopy, measurements, cell counts and statistics

Photomicrographs were obtained using a Leica DM5000B microscope equipped with epifluorescence and a Leica DC500 digital camera. Confocal images were obtained using a Zeiss LSM 510 imaging system at the Hunt-Curtis Imaging Facility at the Ohio State University. Images were optimized for color, brightness and contrast, multiple channels overlaid and figures constructed by using Adobe Photoshop™6.0. Cell counts were performed on representative images. To avoid the possibility of region-specific differences within the retina, cell counts were consistently made from the same region of retina for each data set. Central retina was as assessed within 20° of the posterior pole of the eye, with a linear distance of approximately 1.5 mm. Peripheral retina was considered at approximately

2.5 mm from the peripheral retinal margin, or about 65° eccentric to the posterior pole of the eye. Postnatal chick retina is approximately 13 mm across.

To account for inter-individual variability of eye size, statistical analyses were performed for the differences between measurements of treated and control eyes for each individual. Thus, significance of difference (p-values) for the magnitude of interocular change was calculated for the mean differences from zero by using a two-tailed student's *t*-test. Where significance of difference was determine between two treatment groups without accounting for inter-individual variability we performed a two-tailed student's t-test. Where significance of difference was assessed between experimental groups greater than 2 we performed an ANOVA and a post-hoc Bonferroni test.

2.9. Measurements of eye size

High-resolution A-scan ultrasonography was used to measure corneal thickness, anterior chamber depth, lens thickness and vitreous chamber depth along the optical axis *in vivo*, prior to enucleation. Corneal anesthesia was achieved using one drop of topical 0.5% proparacaine hydrochloride ophthalmic solution. After insertion of a 4mmbarraquer pediatric lid speculum, a 20 MHz Panametrics-NDT (Waltham, MA) transducer with a polystyrene delay line offset (V208-RM) driven by a Panametrics-NDT 5072 pulser-receiver was coupled to the corneal apex using ultrasound coupling gel (Medline Industries, Inc.; Mundelein, IL). The acoustic reflections were collected and digitized using a PicoScope® 5203 USB-PC oscilloscope and the PicoScope® 6 PC Oscilloscope software, version 6.3.43.0. Ultrasonic radio frequency (RF) signals were first filtered with a low-pass filter at the cutoff frequency of 80MHz to exclude high frequency noise. The envelope of the signals was then extracted using the analytic signal magnitude (Gammell 1981). Peaks corresponding to anterior corneal surface and vitreoretinal surface were selected for axial length measurement. Times-of-flight were determined and converted to distance assuming the constant speed of sound of 1540m/s. It is noted that the speed of sound in cornea and lens may be slightly higher that the assumed value. Since the goal of the present study was to compare the thickness and depths between control and treated tissues, the assumption of a uniform speed of sound should have minimal influence on the outcome measures.

Photographs of enucleated eyes were taken using a 6.1 megapixel Nikon D100 SLR camera. High resolution digital images (>50 pixels/mm) of enucleated eyes were measured by using Image Pro Plus 6.2 (Media Cybernetics; Bethesda, MD). Measurements obtained using Image Pro Plus 6.2 were highly reproducible and had low levels of sampling error (± 0.22%) at a resolution of 20 pixels/μm or greater, similar to prior descriptions (Fischer et al. 2009a; Fischer et al. 2010; Ghai et al. 2009). Corneal arc was measured as the linear distance, on profile, across the cornea from ventral limbus to dorsal limbus.

3. Results

3.1. Expression of receptors in different ocular tissues

We sought to examine the expression of receptors for FGF, insulin and IGF1 in different ocular tissues. In a previous study, using RT-PCR, we failed to detect a splice variant of the insulin receptor in retinal cells, whereas this variant was readily detected in the liver (Fischer et al. 2009a). By comparison, using a different set of primers for the insulin receptor, we detect mRNA for the insulin receptor in the choroid+RPE and sclera, whereas faint bands for insulin receptor were detected in the retina, ciliary body and lens (Fig. 1). Similar to the insulin receptor, we detected IGF1R and IGF2R in many different ocular tissues (Fig. 1). Transcripts for IGF1R and IGF2R were detected in the retina, choroid+RPE, lens fiber cells and sclera (Fig. 1). IGF1R was not detected in the ciliary body+lens capsule, whereas

IGF2R was detected (Fig. 1). Our findings are consistent with those of Penha and colleagues which demonstrated expression for insulin receptor and IGF1 receptor in the retina, RPE, choroid and sclera (Penha et al. 2011). All isoforms of the FGF receptor were detected in all tissues of the eye; FGFR1, FGFR2 and FGFR3 were detected in the retina, choroid+RPE, ciliary body, lens and sclera (Fig. 1). Currently, there is no known homologue to FGFR4 in the chick. Each primer set produced a single product at the predicted sizes (see table 1) and PCR products were sequenced to verify the identity. Control reactions excluding the reverse transcriptase for the GAPDH primer set indicated no contamination from genomic DNA.

3.2. Effects of high doses of IGF1 and FGF2 on eye size and retinal integrity

We found that consecutive daily injections of 800ng IGF1 stimulated retinal glia, including Müller glia, microglia and NIRG cells (Fischer et al. 2010). Thus, we began by applying 800ng-doses of IGF1. Unlike the findings of Zhu and Wallman (2009) in which consecutive daily doses of 15 pmol IGF1 increased axial elongation, we found that 3 consecutive daily intraocular injections of 800ng (105 pmol) IGF1 had no significant effect upon ocular growth (difference (treated-control) in axial length 0.04 ± 0.41 mm; p=0.94). By contrast, when 800ng IGF1 was injected with 200ng FGF2 there were significant increases in eye size, including increases in corneal circumference, corneal arc, equatorial circumference and axial length (Figs. 2a–c). These eyes were extremely myopic, with more than minus 20 diopters of refractive error.

We found that retinas were damaged in eyes treated with 800ng IGF1 and 200ng FGF2. *In situ* labeling of fragmented DNA revealed numerous dying cells in the proximal INL and in the GCL in treated eyes (Figs. 3a and 3b). In treated retinas, we found proliferating Sox9-expressing Müller glia that underwent nuclear migration, expressed PCNA, and up-regulated transitin, the avian homologue of mammalian nestin (Figs. 3c–h). Reactive and proliferating Müller glia-derived progenitor cells are known to undergo interkinetic nuclear migration (reviewed by Fischer and Bongini 2010) and transiently up-regulate transitin (Fischer and Omar 2005). Since significant numbers of dying cells were detected in the GCL we probed for the integrity of ganglion cells by immunolabeling for Brn3a (Pou4f2); a POU-domain transcription factor that is expressed by the vast majority of ganglion cells (Xiang et al. 1993). Immunolabeling for Brn3a indicated that treatment with 800ng IGF1 and 200ng FGF2 caused damage and loss of ganglion cells; the remaining ganglion cells appeared atrophic with shrunken nuclei (Figs. 3i and 3j).

3.3. Effects of lower doses of IGF1 and FGF2 on eye size and retinal integrity

The widespread cell death observed with 3 consecutive daily injections of 800ng IGF1 and 200ng FGF2 complicates the interpretation of mechanisms stimulating excessive eye growth. Different types of toxins that destroy retinal neurons are known to cause ocular enlargement (Ehrlich et al. 1990; Fischer et al. 1999b; Fischer et al. 1998; Wildsoet and Pettigrew 1988). Thus, we sought to determine whether lower doses of IGF1 in combination with FGF2 influenced ocular growth. Accordingly, we tested whether 4 consecutive daily intraocular injections of 200ng IGF1 and 200ng FGF2 influenced the size and shape of the eye, and the “health” of retinal cells. Eyes treated with 200ng IGF1 and 200ng FGF2 were significantly larger than contra-lateral control eyes (Figs. 4a and 4b). Measurements from digital images and ultrasonography indicated significant increases in equatorial diameter, axial length, and vitreous chamber depth (Figs. 4c and 4g). In addition, we observed increases in corneal circumference and corneal arc (Fig. 4d). By contrast, ultrasound measurements indicated significant decreases in anterior chamber depth (Figs. 4g); these decreases may have resulted, in part, from thickening of the lens. One day after the last injection of 200ng IGF1 and 200ng FGF2, eyes were extremely myopic with more than minus 20 diopters of refractive error.

We next tested whether the effects of IGF1 and FGF2 on changes in ocular dimensions were transient or long-lasting. IGF1/FGF2-mediated changes in axial length, namely vitreous chamber depth, and equatorial circumference were maintained at 7 days after treatment (Figs. 4e, f and h). These increases in axial length, vitreous chamber depth and equatorial circumference were not significantly different from those seen at 1 day after treatment (compare Figs. 4c,d,g to 4e,f,h). In addition, we found persistent increases in corneal circumference and arc (Fig. 4f): however, these increases were diminished in amplitude compared to those seen at 1 day after treatment (Fig. 4d). By contrast, decreases in anterior chamber depth and increases in lens thickness had disappeared by 7 days after treatment (Fig. 4h). We found that 4 consecutive daily injections of 200ng FGF2 alone have no effects upon ocular growth (difference in axial length (treated-control) 0.08 ± 0.29 mm; p=0.71), consistent with previous reports (Rohrer and Stell 1994). Further, 4 consecutive daily injections of 200ng of IGF1 alone had no effects upon ocular growth (difference in axial length (treated-control) 0.08 ± 0.42 mm; p=0.91), which is not consistent with a previous report (Zhu and Wallman 2009). Similarly, the combination of 1000ng insulin and 200ng FGF2 did not significantly influence ocular size (difference in axial length (treated-control) 0.05 ± 0.37 mm; p=0.78).

One day after the last injection of 200ng IGF1 and 200ng FGF2, we examined the retina and found no indication of cell death (Figs. 5a and 5b), reactivity of Müller glia (Figs. 5c and 5d), or pyknotic ganglion cell nuclei (Figs. 5e and 5f). There was no difference in cell death or glial reactivity in central or peripheral regions of the retina (not shown). We next tested whether injections of 200ng IGF1 and 200ng FGF2 had any long-lasting effects on the retina. At 7 days after the injection, we detected a few scattered TUNEL-positive cells in peripheral regions of the GCL (Figs. 5g and 5h). TUNEL-positive cells were not detected in central regions of treated retinas (data not shown). Consistent with the distribution of TUNEL-positive cells at 7 days after treatment, most (8/10) of the IGF1/FGF2-treated eyes contained regions of peripheral retina that had reduced numbers of Brn3a-positive ganglion cells (Figs. 5i and 5j). By comparison, there was no detectable depletion of Brn3a-positive ganglion cells in central regions of treated retinas (not shown). Seven days after treatment with IGF1 and FGF2, the nuclei of Müller glia were delaminated from the center of the INL (Figs. 5k and 5l). The de-lamination of somata of Müller glia occurs with the reactivity and/or proliferation that can occur with retinal damage or growth factor treatment (reviewed by Fischer and Bongini 2010). Retinas treated with IGF1 alone or FGF2 alone showed no indications of ganglion cell loss or proliferating Müller glia (data not shown), consistent with previous reports (Fischer et al. 2002b; Fischer et al. 2009a; Fischer et al. 2010).

3.4. Effects of IGF1 and FGF2 on the lens, ciliary body and anterior chamber

Eyes treated with IGF1 and FGF2 developed extreme myopic shifts with refractive error in excess of 20 diopters over only 4 days of treatment. Strong myopic reflexes remained for all treated animals corrected with minus 20 diopter lenses. This extreme myopia likely resulted from both increases in vitreous chamber depth and increased refractive power of the lens and/or cornea. To better assess factor-induced changes in the anterior segment, we examined anterior ocular structures in transverse sections at the level of the pupil. Treatment with IGF1 and FGF2 caused angle closure (Figs. 6a,b and g). These changes were apparent in all animals (n=10). Measurements from histological sections revealed that at 7 days after treatment with IGF1 and FGF2 the angle remained significantly narrower compared to the angle of control eyes (Figs. 6c–e and g). However, the mean narrowing of the angle at 7 days after treatment was not as prominent as the narrowing at 1 day after treatment (Figs. 6f and 6g). The inter-animal variability of the angle was large in the treated group (Fig. 6g). In most (7/10) treated animals, we observed significant delamination and putative hypertrophy of the pigmented epithelium of the iris (Fig. 6b). This presumptive hypertrophy of iris

epithelium persisted, in varying degrees between individuals, at 7 days after treatment (compare Figs. 6d and 6e).

IGF1 and FGF's are known to influence lens development, in particular the differentiation of lens fiber cells (reviewed by Lang 1999; McAvoy et al. 1991). Accordingly, we examined whether the lens was affected by treatment with IGF1 and FGF2. Histological observations revealed significant changes in the lens capsule in eyes treated with IGF1 and FGF2 (Figs. 6a–6e). At one day after the last injection of IGF1 and FGF2, the lens capsule of treated eyes appeared abnormal, was filled with vacuoles, and appeared detached from the lens fiber cells (Fig. 6b). At 7 days after the last injection of IGF1 and FGF2, there were persistent changes in the lens which included apparent disorganization among the fiber cells and atrophy of the capsule cells (Figs. 6d and 6e). In most (8/10) of the IGF1/FGF2-treated eyes, an over-growth of non-pigmented epithelial (NPE) cells within the zonules that attached to the lens persisted 7 days after treatment (indicated by arrows in Figs. 6d and 6e). There was significant variability between individuals with respect to persistent changes to the lens and overgrowth of NPE cells (Figs. 6d and 6e).

To better understand IGF1/FGF2-induced changes in the retina, lens and zonules we tested whether proliferation occurred. Proliferating cells were identified by probing for the expression of PCNA and accumulation of BrdU. FGFs have been shown to stimulate the proliferation of progenitors in many different ocular tissues during embryonic development (Chow and Lang 2001). Consistent with previous reports (Fischer et al. 2002a; Fischer and Reh 2000; Fischer and Reh 2003), we found that the combination of IGF1 and FGF2 stimulated the proliferation of progenitors in the CMZ at the peripheral edge of the retina (Figs. 7a and 7b). In eyes treated with IGF1 and FGF2, we did not find a significant induction of proliferation of cells within the iris or anterior lens epithelium (Figs. 7c and 7d). By contrast, we found numerous proliferating cells within equatorial regions of the lens epithelium and within NPE of the ciliary folds that are adjacent to equatorial regions of the lens (Figs. 7e and 7f).

3.5. Effects of IGF1 and FGF2 on intraocular pressure (IOP)

The angle closure observed in IGF1/FGF2-treated eyes (Figs. 6b and 6d) suggested that IOP might be elevated. Accordingly we used a TonoLab^{tm} rebound tonometer to measure IOP in control and treated eyes. IOP measurements were made at 1 day or 7 days after the last injection. In control eyes (n=20) the average IOP was 19.4 ± 3.1 mm Hg. The IOP was not significantly elevated in eyes treated with saline, 300ng IGF1 alone, 200ng FGF2, the combination of insulin and FGF2, or 50ng IGF1 + 200ng FGF2 (Fig. 8). By comparison, the IOP was significantly elevated by approximately 7 mm Hg in eyes treated with 200ng IGF1 + 200ng FGF2 and by approximately 11 mm Hg in eyes treated with 300ng IGF1 + 200ng FGF2 (Fig. 8). Interestingly, the IOP of treated eyes returned to normal levels by 7 days after the last injection (Fig. 8). It must be noted that in treated eyes where the anterior chamber depth has been diminished and the lens is closely opposed to the cornea, the measurements of IOP may not accurately represent the IOP within the eye because of changes in the ability of the cornea to rebound during applanation. Nevertheless, we feel that the measured increases in IOP are representative of increased IOP, but we cannot be certain that the increased IOP was indeed, on average, 11 mm Hg.

3.6. Time course of ocular growth with IGF1/FGF2-treatment

To better understand the development of myopia and ocular dimensions in eyes treated with 200ng IGF1 and 200ng FGF2, we measured refractive error, IOP and ocular dimensions before, during and after treatment. We detected some myopic refractive error 24 hours after the first injection of IGF1 and FGF2 (Fig. 9a). Refractive error was further increased over 2

to 3 days of treatment, with maximal refractive error achieved and maintained at the fourth and fifth days of treatment (Fig. 9a). By comparison, significant increases in IOP, axial length and vitreous chamber depth were not detected until the third day of treatment (Figs. 9b–d). Surprisingly, in this cohort of animals we observed no significant changes in anterior chamber depth or lens thickness at any time during the experiment (Figs. 9e and 9f). These findings emphasize the inter-individual variability of the effects of IGF1 and FGF2 on the lens and anterior chamber.

3.7. Lower dose of IGF1 and FGF2 has some effect on ocular growth

To examine whether lower doses of IGF1 and FGF2 influence refractive state and ocular growth we delivered 4 consecutive daily intraocular injections of 100ng IGF1 and 100ng FGF2. We found that 100ng doses of IGF1 and FGF2 did not influence equatorial circumference, corneal circumference, axial length, vitreous chamber depth, anterior chamber depth or lens thickness (Figs. 10a and 10c). By comparison, we found a small, but significant, increase in myopic refractive error (Fig. 10b), which may have resulted from the increase in corneal arc (Fig. 10c). The effects of 100ng IGF1 and 100ng FGF2 on the lens capsule, ciliary body, iris and ACD was highly variable between individuals. Three out of six treated eyes appeared to have normal ACD, open angle, lens capsule and no hypertrophy of cells in the ciliary body or iris epithelium (Figs. 10h–j). Two of the treated eyes had normal ACD, open angle and iris epithelium, but had dystrophic lens capsule cells, and hypertrophy of cells in the ciliary body (not shown). Only one of the six treated eyes had angle closure, collapse of ACD, dystrophic lens capsule, hypertrophy of iris pigmented epithelium, and hypertrophy of non-pigmented epithelium in the anterior ciliary body (Fig 10k).

4. Discussion

We report here that the combination of IGF1 and FGF2 has a profound influence on ocular growth, the refractive state of the eye, and IOP. The mean increases in axial length were more than 1 mm for 200 ng IGF1 and 200 ng FGF2, compared to increases of nearly 2.5 mm for 800 ng IGF1 and 200 ng FGF2. These IGF1/FGF2-induced increases in eye size over 4 days of treatment are similar to those induced by at least 14 days of form-deprivation (Gottlieb et al. 1987). Neither IGF1 alone, FGF2 alone, nor the combination of insulin and FGF2 influenced axial elongation, refractive error or IOP. Furthermore, we find that the combination of IGF1 and FGF2 stimulates the reactivity of retinal glia, the proliferation of CMZ progenitors, and hypertrophy of NPE cells in the ciliary body. By comparison, the combination of insulin and FGF2 stimulates the reactivity of retinal glia (Fischer et al. 2002b; Fischer et al. 2009a), the proliferation of CMZ progenitors (Fischer et al. 2002a; Fischer and Reh 2000), the hypertrophy of NPE cells in the ciliary body (Fischer and Reh 2003), but not elevated IOP. The precise mechanisms underlying the synergistic activities of IGF1 and FGF2 remain uncertain, and this combination of factors has outcomes distinct from the combination of insulin and FGF2.

We failed to detect significant increases in axial length of eyes injected with IGF1 alone. This is not consistent with a previous report that demonstrated increased axial length, about 0.3 mm, in eyes injected with 68 pmol insulin or 3 consecutive daily doses of 15 pmol IGF1 (Zhu and Wallman, 2010). By comparison, we injected up to 26 pmol and failed to detect increases in vitreous chamber depth or axial elongation. It is possible that subtle differences in injection procedures or strains of chicks underlie these different outcomes. In P7 chicks, serum levels of IGF1 are about 18 ng/ml and levels of insulin are about 0.7 ng/ml (Lu et al. 2007). Therefore, the doses of IGF1 used to influence retinal cells and ocular growth should provide initial maximum concentrations that are about 25–50-fold above serum levels. By comparison, doses of insulin that have been reported to influence ocular growth in open eyes

are between 9,000–21,000-fold above serum levels of insulin (Feldkaemper et al. 2009; Zhu and Wallman 2009). Thus, the doses of IGF1 are biologically more relevant to ocular growth than the tested doses of insulin.

Insulin and IGF1 have similar effects upon retinal cells; activation of microglia, NIRG cells and Müller glia (Fischer et al. 2009a; Fischer et al. 2010). The IGF1 receptor is expressed by cells scattered across the inner retinal layers (IPL and GCL), NIRG cells and/or microglia, but not by cells in the inner and outer nuclear layers (Fischer et al. 2010). With Müller glia, microglia and NIRG cells stimulated by IGF1, there are elevated levels of cell death and wide-spread focal retinal detachments following an excitotoxic insult (Fischer et al. 2010). The increased cell death was prominent within areas of retinal detachment which were coincident with a stark loss of Müller glia and an accumulation of NIRG cells. In the current study, we find evidence for activation of Müller glia by the combination of IGF1 and FGF2; these factors caused the delamination of Müller glia nuclei away from the center of the INL. The presence of Sox9-positive glial nuclei in peripheral regions of the ONL is consistent with the interkinetic nuclear migration and proliferation of Müller glia-derived progenitor-like cells that occurs in response to growth factors (Fischer et al. 2002b; Fischer et al. 2010; Ghai et al. 2010). The actions of IGF1 and FGF2 at extra-retinal cells within the eye remain poorly understood and require further investigation. Our data indicate that receptors for IGF1 and FGF2 are expressed by many different ocular tissues, including the sclera. Furthermore, our data suggest that IGF1/FGF2-induced increases in axial length and vitreous chamber depth are long-lasting; suggesting changes in the sclera. It is also possible some of the long-lasting effects of IGF1 and FGF2 upon the lens, cornea and anterior chamber contribute to sustained increases in refractive error and axial elongation. However, further studies are required to unambiguously determine whether IGF1 and FGF2 act directly on the sclera to enhance ocular elongation.

IGF1/FGF2-induced changes to the cornea, anterior chamber, ciliary body and lens likely contributed to increases in vitreous chamber depth. IGF1/FGF2-treatment caused increases in corneal curvature, decreased anterior chamber depth and a transient increases in lens thickness. However, these changes occurred in only some individuals; IGF1 and FGF2 had highly variably effects between individual on the lens, anterior chamber and ciliary epithelia. The changes to the lens and cornea would have increased refractive power thereby presenting significant plus defocus to the retina. This plus defocus should have stimulated the glucagonergic amacrine cells to produce elevated levels of glucagon peptide to slow rates of ocular growth and thereby decrease vitreous chamber depth (Bitzer and Schaeffel 2002; Feldkaemper and Schaeffel 2002; Fischer et al. 1999a; Vessey et al. 2005). However, our data clearly indicate that eye size was increased, not decreased, by treatment with IGF1 and FGF2. It is possible that the growth-accelerating effects of IGF1/FGF2 override or overwhelm the growth-slowing effects of retinal glucagon. Alternatively, IGF1/FGF2-mediated changes to lens, which included hypertrophy of epithelial cells in equatorial regions of the lens, may have caused significant image blur which should have accelerated rates of ocular growth. Retinoscopy did not indicate significant opacification of the lens, suggesting that IGF1/FGF2-induced changes in the lens may not have form-deprived the retina. Alternatively, lens curvature could have been flattened or density of the fiber cells decreased to reduce refractive power and possibly override changes to anterior chamber and cornea to enhance ocular elongation. We did not assess lens curvature or density in the current study. Thus, it is possible that IGF1/FGF2-mediated changes to the lens degraded the retinal image or flattened the lens to reduce refractive power to enhance rates of ocular growth. However, in one cohort of animals that was treated with 200ng IGF1/FGF2 we did not detect significant changes in ACD or lens thickness, despite significant VCD-elongation and development of refractive error. These findings demonstrate that there is significant inter-individual variability in how anterior ocular tissues respond to IGF1 and FGF2.

Similarly, lower doses (100ng per dose) of IGF1/FGF2 caused a relatively modest shift in refractive error that was accompanied by a significant increase in corneal arc, but no changes in IOP, ACD, VCD or lens thickness. An increase in refractive power in the cornea is expected to result in myopic defocus, and should have caused shortening of the vitreous chamber. However, the lower doses of IGF1/FGF2 had no significant effect on elongation of the vitreous chamber. Similar to the higher doses of IGF1/FGF2, there was significant inter-individual variability with regard to changes in anterior ocular tissues treated with lower doses of IGF1/FGF2.

The sites of action and the retinal cells that are influenced by insulin, IGF1 and FGF2 have recently been investigated. We have reported how insulin and FGF2 influence retinal cells (Fischer et al. 2002b; Fischer et al. 2009a). Insulin and FGF2 induce the phosphorylation of ERK1/2, p38 MAPK and CREB, and the expression of immediate early genes, cFos and Egr1. Accumulations of pERK1/2, p38 MAPK, pCREB, cFos and Egr1 in response to insulin alone or FGF2 alone are confined to Müller glia, whereas retinal neurons do not appear to respond to growth factors. Unlike FGF2, insulin stimulates the reactivity of NIRG cells and microglia (Fischer et al. 2009a). Similar to insulin, IGF1 selectively stimulates Müller glia to accumulate p38 MAPK and cFos, but not pCREB or Egr1, and stimulates the reactivity of NIRG cells and microglia (Fischer et al. 2010). Collectively, our findings indicate that the primary site of action of insulin, IGF1 and FGF2 in the retina are the Müller glia, NIRG cells and microglia. Given that glial proliferation and reactivity results from many different growth factors (Fischer et al. 2009a; Fischer et al. 2009b; Fischer et al. 2010) with no influence on ocular growth, the effects of IGF1 and FGF2 on the retinal glia are unlikely to have any effect upon axial elongation. The identity of extra-retinal cells that are directly influenced by insulin, IGF1 and FGF2 requires further investigation.

It seems likely that rapid, transient increases in IOP resulted from acute angle closure in eyes treated with IGF1 and FGF2. Angle closure is known to be associated with acute increases in IOP (reviewed by Nongpiur et al. 2011). However, we find that significant angle closure persisted for at least 7 days after treatment (Fig. 4h), when IOP returned to normal levels (Fig. 8). This finding suggests that IOP may return to normal levels with a partial opening of the angle and/or that aqueous production was decreased. The mechanisms underlying IGF1/FGF2-induced angle closure remain uncertain. We propose that the hypertrophy of NPE cells adjacent to the lens may cause a lateral expansion and physical, anterior translocation of the ciliary body and iris to close the angle, and thereby transient increase IOP. To the best of our knowledge, there is no precedent for the over-growth of tissues flanking the lens to mechanically close the angle.

It is possible that some of the ocular expansion that we observed in IGF1/FGF2-treated eyes occurs secondary to mechanical pressure imposed by elevated IOP. However, we have not observed increased eye size with increases in IOP induced by injections of polystyrene microbeads into the anterior chamber to inhibit aqueous outflow through the canal of Schlemm (unpublished observations), suggesting that elevated IOP may not be sufficient to drive ocular enlargement in the chick. Conversely, Schmid and colleagues demonstrated that timolol-induced decreases in IOP do not inhibit form deprivation- or lens-induced myopia (Schmid et al. 2000), suggesting that IOP does not influence vision-guided ocular growth. Furthermore, we find that the vitreous chamber of IGF1/FGF2-treated eyes remained enlarged at 7 days after treatment when IOP had returned to normal levels. We propose that the persistent increases in the vitreous chamber of IGF1/FGF2-treated eyes result from remodeling of the sclera. Scleral remodeling likely underlies the long-lasting changes in vitreous chamber elongation (Rada et al. 1998; Rada et al. 2002; Rada et al. 1994). We find that receptors for IGF and FGF are expressed by sclera cells, consistent with the hypothesis that IGF1 and FGF2 may be acting directly on the sclera. A recent report by Penha and

colleagues (Penha et al. 2011) has demonstrated that IGF1R is expressed by sclera cells and that expression levels are up-regulated with growth-enhancing minus defocus. Thus, we propose that long-lasting increases in the size of the vitreous chamber results from changes to the sclera, and that IGF1 and FGF2 may act directly on sclera cells.

In eyes treated with IGF1 and FGF2 we observed ocular enlargement and elevated IOP, and at some time between 1 and 7 days after treatment IOP returned to normal, ganglion cells were lost from peripheral regions of the retina and the Müller glia became reactive. In glaucomatous eyes, the loss of ganglion cells is prevalent and begins in peripheral regions of the retina. Reports indicate that ganglion cells in peripheral regions of the retina are more susceptible than those found in central regions of the retina to increases in IOP (reviewed by Qu et al. 2010). It remains uncertain whether the loss of ganglion cells in IGF1/FGF2-treated retinas result directly from elevated IOP or other effects, such as glial reactivity. However, glial reactivity likely follows the loss of ganglion cells in peripheral retinal regions seen at 7 days after treatment and likely resulted from elevated IOP that persisted beyond 1 day after treatment with IGF1 and FGF2. Alternatively, factor-induced activation of microglia could influence the survival of ganglion cells. For example, IGF1 is known to stimulate retinal microglia (Fischer et al. 2010) and activated microglia may have detrimental effects upon the survival of ganglion cells in different models of optic nerve damage (Huang et al. 2007; Nakazawa et al. 2007). It is unlikely that the loss of ganglion cells in peripheral retinal regions influences ocular growth given that significant growth occurred before the loss ganglion cells and reports have indicated that ganglion cells are not required for vision-guided ocular growth (McBrien et al. 1995; Norton et al. 1994; Troilo et al. 1987; Wildsoet 2003).

Conclusions

Our findings indicate that the combination of IGF1 and FGF2, but neither factor alone, had a significant impact upon myopic development, ocular enlargement, angle closure, elevated IOP and retinal damage. Our findings indicate that IGF1 and FGF2 act at multiple sites within the eye to influence eye growth, IOP and neuronal survival in the retina. We conclude that IGF1 and FGF2 act synergistically to have profound transient effects upon IOP, and long-lasting effects upon vitreous chamber elongation, angle closure, lens integrity and myopic refractive error. The ocular elongation that occurs with IGF1/FGF2 treatment likely results from combined effects upon sclera growth, lens pathology, changes to the ciliary body, and corneal changes.

Acknowledgments

We thank Dr. Don Mutti for providing comments that contributed to final form of the manuscript. We thank Dr. Andy Hartwick for providing assistance with measurements of intraocular measure. We thank Drs. Paul Henion and Paul Linser for providing antibodies to transitin and 2M6, respectively. The antibodies developed by Drs. S.J. Kaufman (BrdU), D.M. Fambrough (Lysosomal membrane glycoprotein), and G. Cole (transitin) were obtained from the Developmental Studies Hybridoma Bank, which was developed under the auspices of the NICHD and is maintained by the University of Iowa, Department of Biological Sciences, Iowa City, IA 52242. Confocal microscopy was performed at the Hunt-Curtis Imaging Facility at the Department of Neuroscience of The Ohio State University. This work was supported by grants (AJF: EY016043-05; ERR: K12EY015447) from the National Institutes of Health, National Eye Institute.

References

Bitzer M, Schaeffel F. Defocus-induced changes in ZENK expression in the chicken retina. Invest Ophthalmol Vis Sci. 2002; 43(1):246–52. [PubMed: 11773038]

Buck C, Schaeffel F, Simon P, Feldkaemper M. Effects of positive and negative lens treatment on retinal and choroidal glucagon and glucagon receptor mRNA levels in the chicken. Invest Ophthalmol Vis Sci. 2004; 45(2):402–9. [PubMed: 14744878]

Chaum E. Retinal neuroprotection by growth factors: a mechanistic perspective. J Cell Biochem. 2003; 88(1):57–75. [PubMed: 12461775]

Chow RL, Lang RA. Early eye development in vertebrates. Annu Rev Cell Dev Biol. 2001; 17:255–96. [PubMed: 11687490]

Ehrlich D, Sattayasai J, Zappia J, Barrington M. Effects of selective neurotoxins on eye growth in the young chick. Ciba Found Symp. 1990; 155:63–84. discussion 84–8. [PubMed: 2088682]

Feldkaemper MP, Neacsu I, Schaeffel F. Insulin acts as a powerful stimulator of axial myopia in chicks. Invest Ophthalmol Vis Sci. 2009; 50(1):13–23. [PubMed: 18599564]

Feldkaemper MP, Schaeffel F. Evidence for a potential role of glucagon during eye growth regulation in chicks. Vis Neurosci. 2002; 19(6):755–66. [PubMed: 12688670]

Fischer AJ, Bongini R. Turning Muller glia into neural progenitors in the retina. Mol Neurobiol. 2010; 42(3):199–209. [PubMed: 21088932]

Fischer AJ, Dierks BD, Reh TA. Exogenous growth factors induce the production of ganglion cells at the retinal margin. Development. 2002a; 129(9):2283–91. [PubMed: 11959835]

Fischer AJ, Foster S, Scott MA, Sherwood P. Transient expression of LIM-domain transcription factors is coincident with delayed maturation of photoreceptors in the chicken retina. J Comp Neurol. 2008a; 506(4):584–603. [PubMed: 18072193]

Fischer AJ, McGuire CR, Dierks BD, Reh TA. Insulin and fibroblast growth factor 2 activate a neurogenic program in Muller glia of the chicken retina. J Neurosci. 2002b; 22(21):9387–98. [PubMed: 12417664]

Fischer AJ, McGuire JJ, Schaeffel F, Stell WK. Light- and focus-dependent expression of the transcription factor ZENK in the chick retina. Nat Neurosci. 1999a; 2(8):706–12. [PubMed: 10412059]

Fischer AJ, Morgan IG, Stell WK. Colchicine causes excessive ocular growt and myopia in chicks. Vision Res. 1999b; 39(4):685–97. [PubMed: 10341956]

Fischer AJ, Omar G. Transitin, a nestin-related intermediate filament, is expressed by neural progenitors and can be induced in Muller glia in the chicken retina. J Comp Neurol. 2005; 484(1): 1–14. [PubMed: 15717308]

Fischer AJ, Reh TA. Identification of a proliferating marginal zone of retinal progenitors in postnatal chickens. Dev Biol. 2000; 220(2):197–210. [PubMed: 10753510]

Fischer AJ, Reh TA. Growth factors induce neurogenesis in the ciliary body. Dev Biol. 2003; 259(2): 225–40. [PubMed: 12871698]

Fischer AJ, Ritchey ER, Scott MA, Wynne A. Bullwhip neurons in the retina regulate the size and shape of the eye. Dev Biol. 2008b; 317(1):196–212. [PubMed: 18358467]

Fischer AJ, Scott MA, Ritchey ER, Sherwood P. Mitogen-activated protein kinase-signaling regulates the ability of Müller glia to proliferate and protect retinal neurons against excitotoxicity. Glia. 2009a; 57(14):1538–1552. [PubMed: 19306360]

Fischer AJ, Scott MA, Tuten W. Mitogen-activated protein kinase-signaling stimulates Muller glia to proliferate in acutely damaged chicken retina. Glia. 2009b; 57(2):166–81. [PubMed: 18709648]

Fischer AJ, Scott MA, Zelinka C, Sherwood P. A novel type of glial cell in the retina is stimulated by insulin-like growth factor 1 and may exacerbate damage to neurons and Muller glia. Glia. 2010; 58(6):633–49. [PubMed: 19941335]

Fischer AJ, Seltner RL, Stell WK. Opiate and N-methyl-D-aspartate receptors in form-deprivation myopia. Vis Neurosci. 1998; 15(6):1089–96. [PubMed: 9839973]

Gammell PM. Improved ultrasonic detection using the analytic signal magnitude. Ultrasonics. 1981; 19(2):73–76.

Ghai K, Zelinka C, Fischer AJ. Serotonin released from amacrine neurons is scavenged and degraded in bipolar neurons in the retina. J Neurochem. 2009; 111(1):1–14. [PubMed: 19619137]

Ghai K, Zelinka C, Fischer AJ. Notch signaling influences neuroprotective and proliferative properties of mature Muller glia. J Neurosci. 2010; 30(8):3101–12. [PubMed: 20181607]

Gottlieb MD, Fugate-Wentzek LA, Wallman J. Different visual deprivations produce different ametropias and different eye shapes. Invest Ophthalmol Vis Sci. 1987; 28(8):1225–35. [PubMed: 3610540]

Guo SS, Sivak JG, Callender MG, Diehl-Jones B. Retinal dopamine and lens-induced refractive errors in chicks. Curr Eye Res. 1995; 14(5):385–9. [PubMed: 7648864]

Hicks D. Putative functions of fibroblast growth factors in retinal development, maturation and survival. Semin Cell Dev Biol. 1998; 9(3):263–9. [PubMed: 9665861]

Huang Y, Li Z, van Rooijen N, Wang N, Pang CP, Cui Q. Different responses of macrophages in retinal ganglion cell survival after acute ocular hypertension in rats with different autoimmune backgrounds. Exp Eye Res. 2007; 85(5):659–66. [PubMed: 17825287]

Lang RA. Which factors stimulate lens fiber cell differentiation in vivo? Invest Ophthalmol Vis Sci. 1999; 40(13):3075–8. [PubMed: 10586926]

LaVail MM, Yasumura D, Matthes MT, Lau-Villacorta C, Unoki K, Sung CH, Steinberg RH. Protection of mouse photoreceptors by survival factors in retinal degenerations. Invest Ophthalmol Vis Sci. 1998; 39(3):592–602. [PubMed: 9501871]

Lu JW, McMurtry JP, Coon CN. Developmental changes of plasma insulin, glucagon, insulin-like growth factors, thyroid hormones, and glucose concentrations in chick embryos and hatched chicks. Poult Sci. 2007; 86(4):673–83. [PubMed: 17369538]

McAvoy JW, Chamberlain CG, de Iongh RU, Richardson NA, Lovicu FJ. The role of fibroblast growth factor in eye lens development. Ann N Y Acad Sci. 1991; 638:256–74. [PubMed: 1723855]

McBrien NA, Moghaddam HO, Cottriall CL, Leech EM, Cornell LM. The effects of blockade of retinal cell action potentials on ocular growth, emmetropization and form deprivation myopia in young chicks. Vision Res. 1995; 35(9):1141–52. [PubMed: 7610575]

Metlapally R, Ki CS, Li YJ, Tran-Viet KN, Abbott D, Malecaze F, Calvas P, Mackey DA, Rosenberg T, Paget S, et al. Genetic association of insulin-like growth factor-1 polymorphisms with high-grade myopia in an international family cohort. Invest Ophthalmol Vis Sci. 2010; 51(9):4476–9. [PubMed: 20435602]

Morrison JC, Jia L, Cepurna W, Guo Y, Johnson E. Reliability and sensitivity of the TonoLab rebound tonometer in awake Brown Norway rats. Invest Ophthalmol Vis Sci. 2009; 50(6):2802–8. [PubMed: 19324849]

Nakazawa T, Hisatomi T, Nakazawa C, Noda K, Maruyama K, She H, Matsubara A, Miyahara S, Nakao S, Yin Y, et al. Monocyte chemoattractant protein 1 mediates retinal detachment-induced photoreceptor apoptosis. Proc Natl Acad Sci U S A. 2007; 104(7):2425–30. [PubMed: 17284607]

Nongpiur ME, Ku JY, Aung T. Angle closure glaucoma: a mechanistic review. Curr Opin Ophthalmol. 2011; 22(2):96–101. [PubMed: 21252671]

Norton TT. Experimental myopia in tree shrews. Ciba Found Symp. 1990; 155:178–94. discussion 194-9. [PubMed: 2088676]

Norton TT, Essinger JA, McBrien NA. Lid-suture myopia in tree shrews with retinal ganglion cell blockade. Vis Neurosci. 1994; 11(1):143–53. [PubMed: 8011577]

Pease ME, Cone FE, Gelman S, Son JL, Quigley HA. Calibration of the TonoLab Tonometer in Mice with Spontaneous or Experimental Glaucoma. Invest Opthaimol Vis Sci. 2010

Penha AM, Schaeffel F, Feldkaemper M. Insulin, insulin-like growth factor-1, insulin receptor, and insulin-like growth factor-1 receptor expression in the chick eye and their regulation with imposed myopic or hyperopic defocus. Mol Vis. 2011; 17:1436–48. [PubMed: 21655358]

Qu J, Wang D, Grosskreutz CL. Mechanisms of retinal ganglion cell injury and defense in glaucoma. Exp Eye Res. 2010; 91(1):48–53. [PubMed: 20394744]

Rada JA, Achen VR, Rada KG. Proteoglycan turnover in the sclera of normal and experimentally myopic chick eyes. Invest Ophthalmol Vis Sci. 1998; 39(11):1990–2002. [PubMed: 9761277]

Rada JA, Johnson JM, Achen VR, Rada KG. Inhibition of scleral proteoglycan synthesis blocks deprivation-induced axial elongation in chicks. Exp Eye Res. 2002; 74(2):205–15. [PubMed: 11950231]

Rada JA, Matthews AL, Brenza H. Regional proteoglycan synthesis in the sclera of experimentally myopic chicks. Exp Eye Res. 1994; 59(6):747–60. [PubMed: 7698268]

Rohrer B, Stell WK. Basic fibroblast growth factor (bFGF) and transforming growth factor beta (TGF-beta) act as stop and go signals to modulate postnatal ocular growth in the chick. Exp Eye Res. 1994; 58(5):553–61. [PubMed: 7925692]

Schmid KL, Abbott M, Humphries M, Pyne K, Wildsoet CF. Timolol lowers intraocular pressure but does not inhibit the development of experimental myopia in chick. Exp Eye Res. 2000; 70(5):659–66. [PubMed: 10870524]

Tarutta E, Chua WH, Young T, Goldschmidt E, Saw SM, Rose KA, Smith E 3rd, Mutti DO, Ashby R, Stone RA, et al. Myopia: Why Study the Mechanisms of Myopia? Novel Approaches to Risk Factors Signaling Eye Growth- How Could Basic Biology Be Translated into Clinical Insights? Where Are Genetic and Proteomic Approaches Leading? How Does Visual Function Contribute to and Interact with Ametropia? Does Eye Shape Matter? Why Ametropia at All? Optom Vis Sci. 2011; 88(3):404–447.

Tejedor J, de la Villa P. Refractive changes induced by form deprivation in the mouse eye. Invest Ophthalmol Vis Sci. 2003; 44(1):32–6. [PubMed: 12506052]

Troilo D, Gottlieb MD, Wallman J. Visual deprivation causes myopia in chicks with optic nerve section. Curr Eye Res. 1987; 6(8):993–9. [PubMed: 3665562]

Troilo D, Judge SJ. Ocular development and visual deprivation myopia in the common marmoset (Callithrix jacchus). Vision Res. 1993; 33(10):1311–24. [PubMed: 8333155]

Valter K, Maslim J, Bowers F, Stone J. Photoreceptor dystrophy in the RCS rat: roles of oxygen, debris, and bFGF. Invest Ophthalmol Vis Sci. 1998; 39(12):2427–42. [PubMed: 9804151]

Vessey KA, Lencses KA, Rushforth DA, Hruby VJ, Stell WK. Glucagon receptor agonists and antagonists affect the growth of the chick eye: a role for glucagonergic regulation of emmetropization? Invest Ophthalmol Vis Sci. 2005; 46(11):3922–31. [PubMed: 16249465]

Wallman J, Turkel J, Trachtman J. Extreme myopia produced by modest change in early visual experience. Science. 1978; 201(4362):1249–51. [PubMed: 694514]

Wallman J, Winawer J. Homeostasis of eye growth and the question of myopia. Neuron. 2004; 43(4): 447–68. [PubMed: 15312645]

Wiesel TN, Raviola E. Myopia and eye enlargement after neonatal lid fusion in monkeys. Nature. 1977; 266(5597):66–8. [PubMed: 402582]

Wildsoet C. Neural pathways subserving negative lens-induced emmetropization in chicks--insights from selective lesions of the optic nerve and ciliary nerve. Curr Eye Res. 2003; 27(6):371–85. [PubMed: 14704921]

Wildsoet CF, Pettigrew JD. Kainic acid-induced eye enlargement in chickens: differential effects on anterior and posterior segments. Invest Ophthalmol Vis Sci. 1988; 29(2):311–9. [PubMed: 3338888]

Xiang M, Zhou L, Peng YW, Eddy RL, Shows TB, Nathans J. Brn-3b: a POU domain gene expressed in a subset of retinal ganglion cells. Neuron. 1993; 11(4):689–701. [PubMed: 7691107]

Zhu X, Wallman J. Opposite effects of glucagon and insulin on compensation for spectacle lenses in chicks. Invest Ophthalmol Vis Sci. 2009; 50(1):24–36. [PubMed: 18791176]

Highlights

- We investigate how the combination of IGF1 and FGF2 influence rates of ocular growth.
- Treated eyes had increased equatorial diameter and vitreous chamber depth.
- Treated eyes developed myopia, in excess of 15 diopters of refractive error.
- There were variable effects upon angle closure, intraocular pressure, lens epithelium hypertrophy, narrowing of the anterior chamber, and hypertrophy of ciliary epithelia.

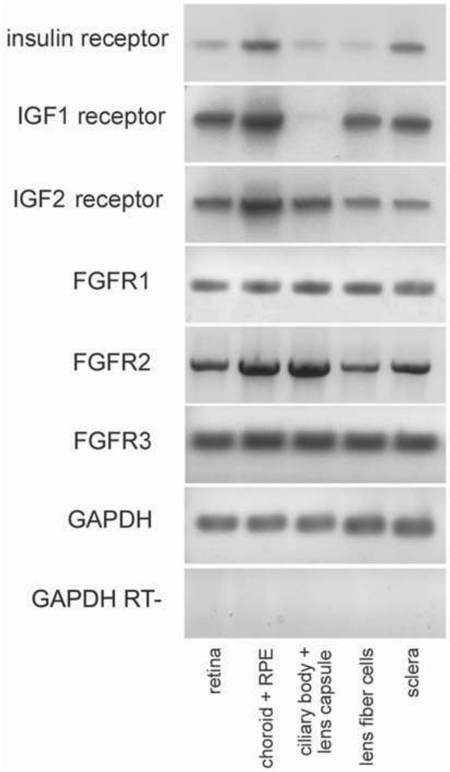

Figure 1.

Receptors to insulin, IGF and FGF are widely expressed in different ocular tissues. RT-PCR was used to detect transcripts to the insulin receptor, IGF1 receptor, IGF2 receptor, FGFR1, FGFR2 and FGFR3. PCR was performed on cDNA pools obtained from retina, choroid +RPE, ciliary body+lens capsule, lens fiber cells and sclera. Abbreviations: FGFR – fibroblast growth factor receptor, IGF – insulin-like growth factor, GAPDH - Glyceraldehyde 3-phosphate dehydrogenase, RPE – retinal pigmented epithelium.

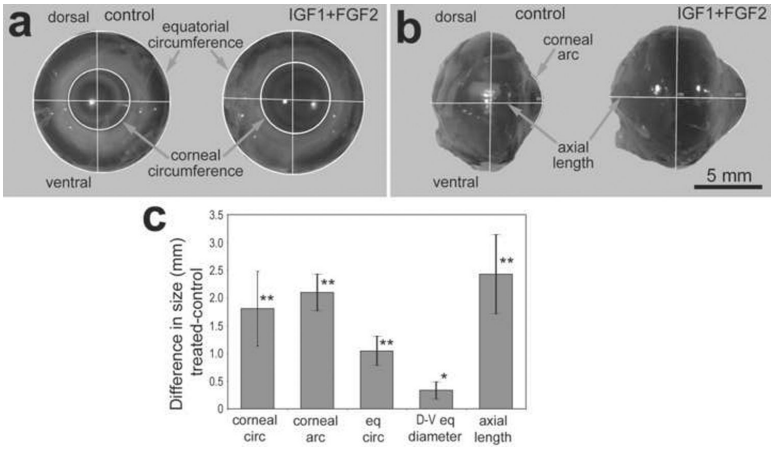

Figure 2.

Three consecutive daily intraocular injections of 800ng IGF1 and 200ng FGF2 stimulate excessive ocular growth. Injections began at P5, ended at P7, and measurements were performed on enucleated eyes at P8 (paradigm 1). Measurements of enucleated eyes were made from digital images using ImagePro6.2. Measurements of eyes (n=6) were made on axis (**a**) and on profile (**b**). The histogram illustrates the mean (±SD) difference in ocular dimension (mm; **c**). Measurements included corneal circumference (corneal circ), corneal arc, equatorial circumference (eq circ), dorsal-ventral equatorial diameter (D–V eq diameter), and axial length. Statistical significance (*p<0.05, **p<0.001, n=6) was determined by using a paired, two-tailed student's t-test.

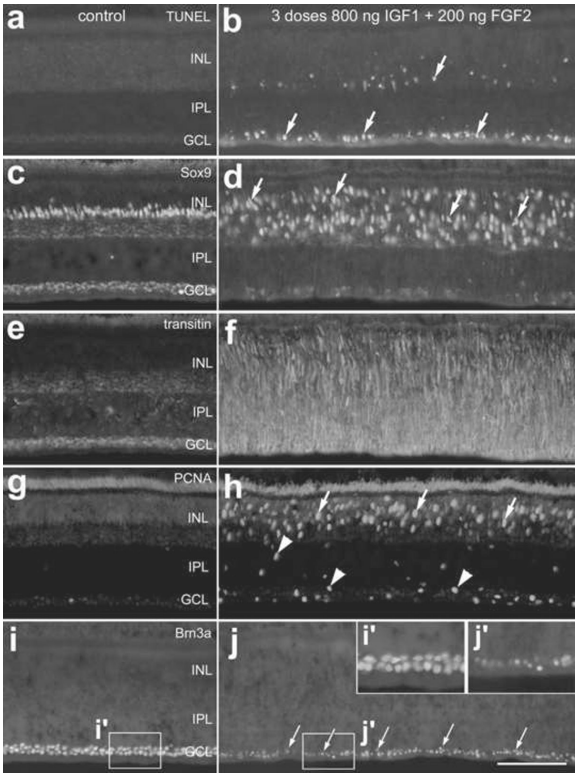

Figure 3.

Treatment with 3 consecutive daily injections of 800ng IGF1 and 200ng FGF2 causes cell death, glial migration and proliferation within the retina. Retinas were harvested 1 day after the last of 3 consecutive daily injections of factors (paradigm 1). Vertical sections of central regions of the retina were labeled for fragmented DNA using the TUNEL method (**a** and **b**) or with antibodies to Sox9 (**c** and **d**), transitin (**e** and **f**), PCNA (**g** and **h**) or Brn3a (**I** and **j**). Arrows indicate dying cells (**b**), reactive Müller glia (**d**), proliferating Müller glia (**h**) or abnormal ganglion cell nuclei (**j**). Arrow-heads indicate putative NIRG cells that are PCNA-positive (**h**). The insets (**i'** and **j'**) in panel **j** are 2-fold enlargements of the boxed-out regions in **i** and **j**. The calibration bar (50 μm) in panel **j** applies to all panels. Abbreviations: INL – inner nuclear layer, IPL – inner plexiform layer, GCL – ganglion cell layer, PCNA – proliferating cell nuclear antigen.

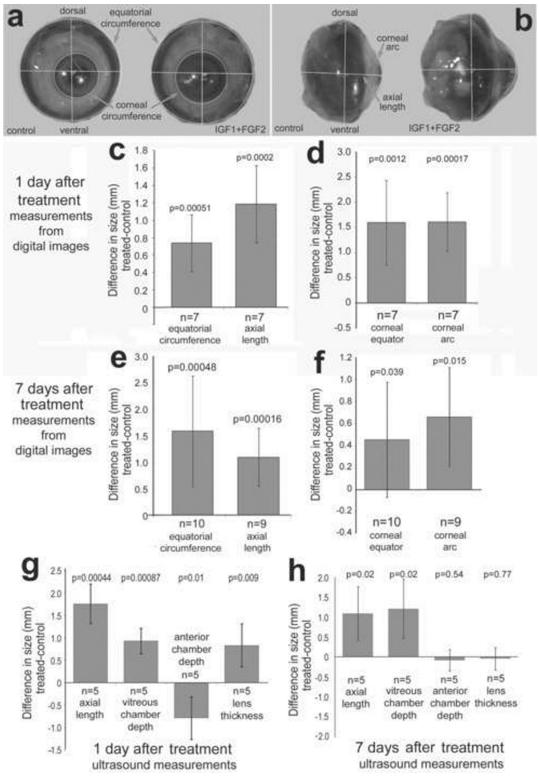

Figure 4.

Four consecutive daily intraocular injections of 200ng IGF1 and 200ng FGF2 stimulate excessive ocular growth. Injections began at P5, ended at P8, and ocular measurements were performed at P9 (paradigm 2; **a**–**d** and **g**) or P16 (paradigm 3; **e**,**f** and **h**). Measurements were made by using ImagePro6.2 on digital images of enucleated eyes (**a**–**f**) and by using A-scan ultrasonography (**g** and **h**). Histograms represent the mean and standard deviation for data-sets. Measurements using ImagePro6.2 included nasal-temporal equatorial diameter (N–T diameter), dorsal-ventral equatorial diameter (D–V diameter), equatorial circumference, axial length, corneal circumference, and corneal arc. Measurements using A-scan ultrasound included axial length, vitreous chamber depth, anterior chamber depth and lens thickness. Statistical significance was determined by using a paired, two-tailed student's t-test.

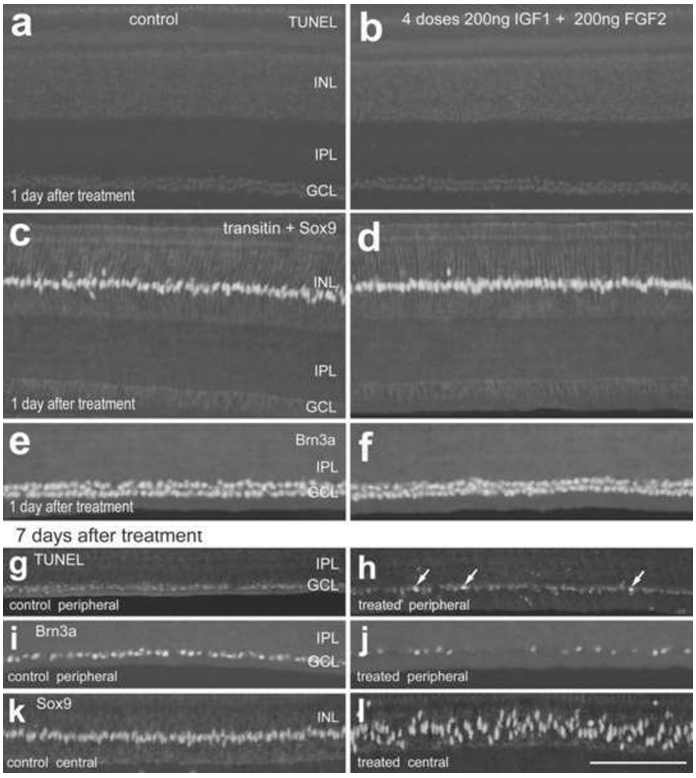

Figure 5.

Four consecutive daily intraocular injections of 200ng IGF1 and 200ng FGF2 do not have short-term effects upon cell death, glial reactivity or the integrity of ganglion cells, whereas the long-term survival of ganglion cells in the peripheral retina is compromised. Injections of IGF1 and FGF2 began at P5, ended at P8, and tissues were harvested at P9 (paradigm 2; **a**–**f**) or P15 (paradigm 3; **g**–**l**). Vertical sections of control (**a**,**c**,**e**,**g**,**i** and **k**) and treated retinas (**b**,**d**,**f**,**h**,**j** and **l**) were labeled for TUNEL (**a**,**b**,**g** and **h**), Sox9 (**c**,**d** and **k**–**l**), transitin (**c** and **d**), and Brn3a (**e**,**f**,**i** and **j**). Arrows indicate labeled nuclei. The calibration bar (50 μm) in panel **n** applies to all panels. Abbreviations: INL – inner nuclear layer, IPL – inner plexiform layer, GCL – ganglion cell layer.

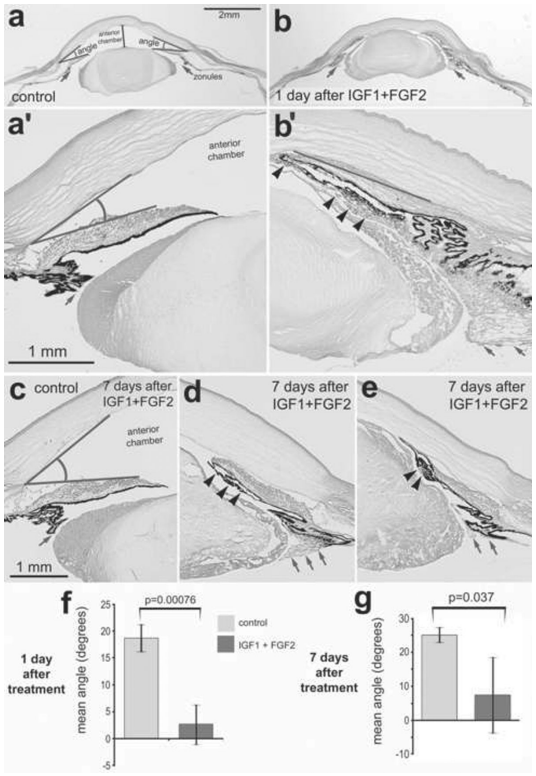

Figure 6.

Four consecutive daily intraocular injections of 200ng IGF1 and 200ng FGF2 dramatically change the anterior segment of the eye. Sections were obtained from control eyes (**a** and **c**) and from eyes treated with IGF1 and FGF2 (**b**, **d** and **e**) and were stained with hematoxylin and eosin. Injections began at P5, ended at P8, and ocular measurements were performed at P9 (paradigm 2; **a**, **b** and **f**) or P16 (paradigm 3; **c**–**e** and **g**). The arrows indicate the zonules that attach to the lens, straight lines indicate the angle, and arrow-heads indicate delaminated iris epithelium. Histograms indicate the mean and standard deviation for the angle (degrees; **f** and **g**). Significance of difference (*p*-value) was determined using a two-tailed student *t*-test.

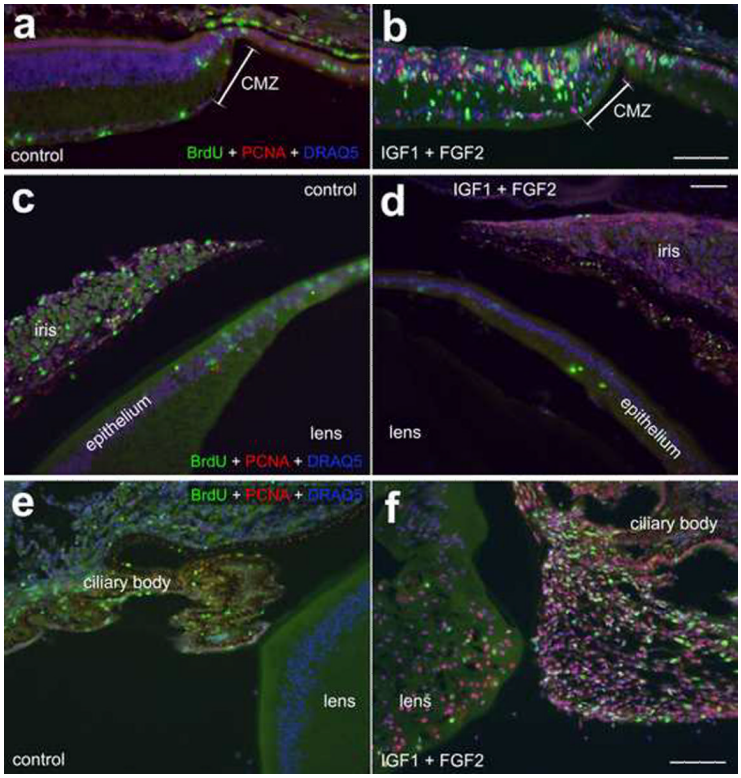

Figure 7.

Intraocular injections of 200ng IGF1 and 200ng FGF2 stimulate the proliferation of cells in far peripheral regions of the retina, progenitors in the CMZ, equatorial regions of lens capsule, and non-pigmented epithelial cells in the zonules. Sections were labeled with DRAQ5 (nuclei; blue), PCNA (red) and BrdU (green). Sections were obtained from control eyes (paradigm 2; **a**, **c** and **e**) and eyes 1 day after the last of 4 consecutive daily injections of IGF1 and FGF2 (paradigm 2; **b**, **d** and **f**). The calibration bar (50 μm) in panel **b** applies to panels **a** and **b**, the bar in **d** applies to **c** and **d**, and the bar in **f** applies to **e** and **f**. Abbreviations: CMZ – circumferential marginal zone, PCNA – proliferating cell nuclear antigen.

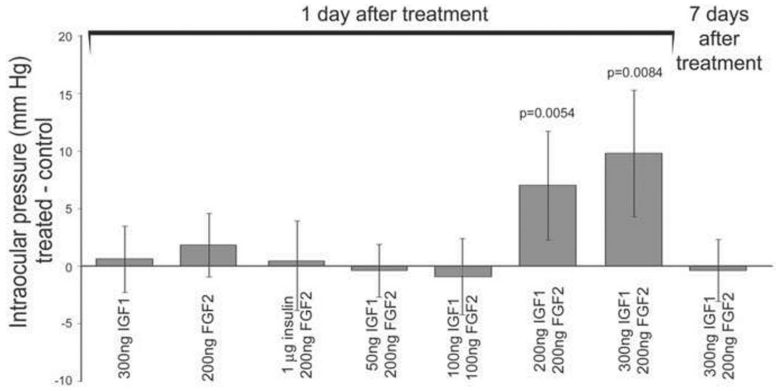

Figure 8.

Intraocular injections of the combination of IGF1 and FGF2 increase intraocular pressure (IOP) in a dose-dependent manner. Histograms indicate the mean and standard deviation for the IOP of eyes treated with 4 consecutive daily doses of 300ng IGF1 alone, 200ng FGF2 alone, 1μg insulin + 200ng FGF2, 50ng IGF1 + 200ng FGF2, 100ng IGF1 + 100ng FGF2, 200ng IGF1 + 200ng FGF2, or 300ng IGF1 + 200ng FGF2 (paradigm 6). IOP measurements were made at 1 or 7 days after the last injection. Significance of difference was performed using ANOVA ($p<0.0001$), two-tailed student's t-test to assess significance at each time or treatment, and a post-hoc two-way Bonferroni test was used to determine the significance of difference ($p=0.002$) between 1 and 7 days after treatment with 300ng IGF1 and 200ng FGF2.

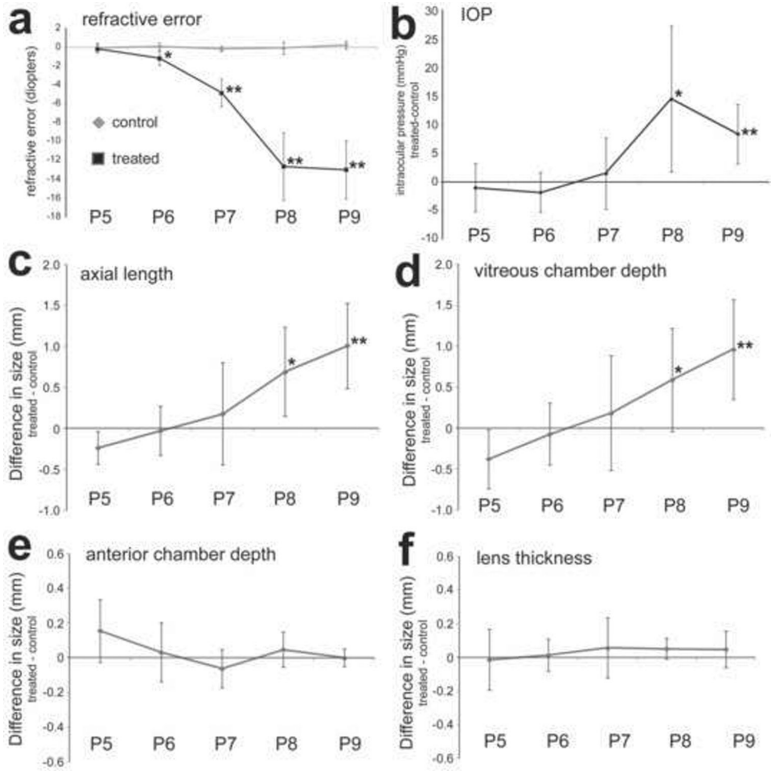

Figure 9.

Consecutive daily intraocular injections of 200ng IGF1 and 200ng FGF2 stimulate excessive ocular growth progressively over 4 days. Injections began at P5, ended at P8. Ocular measurements were performed at P5, P6, P7, P8 and P9 (paradigm 4; n=6). Measurements were made by using streak retinoscopy (**a**), a Tonolab tonometer (**b**), and A-scan ultrasonography (**c–f**). Ultrasound measurements include axial length (**c**), vitreous chamber depth (**d**), anterior chamber depth (**e**) and lens thickness (**f**). Histograms represent the mean and standard deviation for data-sets. Measurements using A-scan ultrasound included axial length, vitreous chamber depth, anterior chamber depth and lens thickness. Statistical significance (*p<0.05 and **p<0.005) was determined by using two-way ANOVA and was followed by a post-hoc, two-tailed student's t-test.

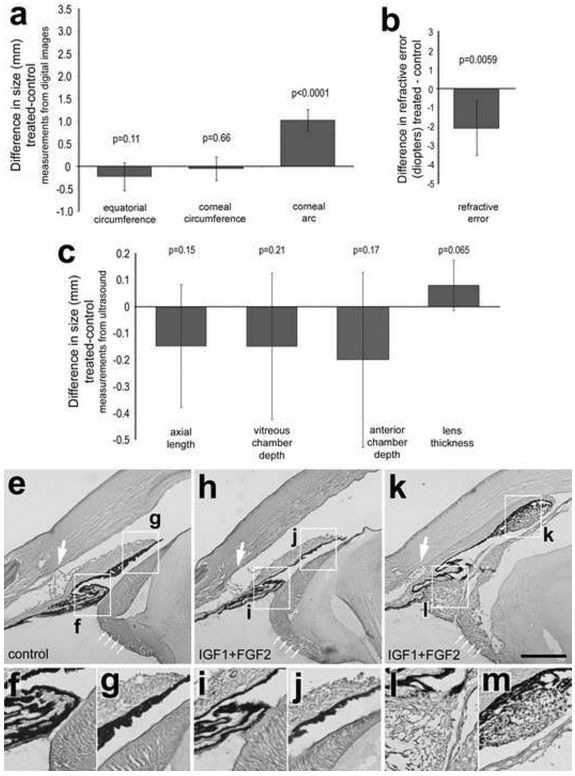

Figure 10.

Four consecutive daily intraocular injections of 100ng IGF1 and 100ng FGF2 do not stimulate excessive ocular elongation. Injections began at P5, ended at P8, and ocular measurements were performed at P9 (paradigm 5; n=6). Measurements were made by using ImagePro6.2 on digital images of enucleated eyes (**a**), streak retinoscopy (**b**), and A-scan ultrasonography (**c**). Histograms represent the mean and standard deviation for data-sets. Measurements using ImagePro6.2 included equatorial circumference, corneal circumference, and corneal arc. Measurements using A-scan ultrasound included axial length, vitreous chamber depth, anterior chamber depth and lens thickness. Hematoxylin and Eosin-stained sections through anterior ocular structures included a control eye (**e–g**), a treated eye exhibiting no significant IGF1/FGF2-mediated effects (**h–j**), and a treated eye exhibiting significant hypertrophy of cells in the ciliary body, lens capsule and iris epithelium (**k–m**). The boxed-out areas in panels **e**, **h** and **k** are enlarged 2-fold in the panels immediately below. Statistical significance was determined by using a paired, two-tailed student's t-test.

Table 1

PCR primers (5' to 3'), target and predicted product sizes:

Target mRNA	Sequence	Product size (bp)	Annealing temperature
Insulin receptor	forward TTG CCA TAA TCA TTG CTG GA reverse CCT CTG TTT CCA GAG GCT TG	1065	64.7°C
IGF1 receptor	forward GGC AAA GCT GAC ACA TCT GA reverse TCC AGG TCA AGC TCC TCT GT	1221	60°C
IGF2 receptor	forward GCT GGA TGT GAA GCA GAC AA reverse GCC TCC CAG TTC TCT CTG TG	1199	60°C
FGFR1	forward ATA ACA CCA AGC CGA ACC AG reverse GGC AGC TCA TAC TCG GAG AC	970	60°C
FGFR2	forward GCT GTC CAC AAG CTG ACA AA reverse GGT GCA GTT GGC AGG TTT AT	948	60°C
FGFR3	forward TTG GCC TTG CTA GAG ACG TT reverse AGG GCA GTA CCC TCA GGT TT	854	60°C
GAPDH	forward GGA ACA CTA TAA AGG CGA GAT reverse TCA CAA GTT TCC CGT TCT CA	218	60°C

Table 2

Antibodies, sources and working dilutions.

Antigen	Working dilution	Host	Clone or catalog number	Source
Sox9	1:2000	rabbit	AB5535	Millipore Billerica, MA
Brn3a (Pou4f2)	1:200	mouse	mab1585	Millipore Billerica, MA
transitin	1:80	mouse	EAP3	Developmental Studies Hybridoma Bank (DSHB) Iowa City, IA
TopAP	1:100	mouse	2M6	Dr. P. Linser University of Florida[31]
Cleaved caspase 3	1:500	rabbit	AF583	R&D Systems Minneapolis, MN
Proliferating cell nuclear antigen	1:1000	mouse	M0879	Dako Immunochemicals Carpinteria, CA
BrdU	1:200	rat	OBT00030S	AbD Serotec Raleigh, NC
BrdU	1:100	mouse	G3G4	DSHB